Scientia Iranica D (2012) 19 (3), 745–758

Sharif University of Technology

Scientia Iranica

Transactions D: Computer Science & Engineering and Electrical Engineering

www.sciencedirect.com

Social welfare maximization with fuzzy based genetic algorithm by TCSC and SSSC in double-sided auction market

S.M.H. Nabavi [a], **A. Kazemi** [a,*], **M.A.S. Masoum** [b]

[a] *Department of Electrical Engineering, Iran University of Science and Technology, Tehran, Iran*
[b] *Department of Electrical and Computer Engineering, Curtin University of Technology, Perth, WA, Australia*

Received 28 August 2010; revised 5 February 2011; accepted 11 April 2011

KEYWORDS

Congestion management;
Social welfare;
Double-sided auction market;
Generator and load rescheduling;
SSSC and TCSC;
Fuzzy and GA.

Abstract This paper presents a fuzzy-based genetic algorithm to maximize total system social welfare by best the placement and sizing of TCSC and SSSC devices, considering their investment cost in a double-sided auction market. To introduce more accurate modeling, the valve loading effects are incorporated into the conventional quadratic smooth generator cost curves. In addition, quadratic consumer benefit functions are integrated into the objective function to guarantee that locational marginal prices charged at the demand buses are less than, or equal to, the DisCos benefit, earned by selling the power to retail customers. The proposed approach utilizes fuzzy-based genetic algorithms for optimal scheduling of GenCos and DisCos, as well as optimal placement and sizing of SSSC and TCSC units. In addition, the Newton–Raphson approach is used to minimize the mismatch of the power flow equation. Simulation results on the modified IEEE 14-bus and IEEE 30-bus test systems (with/without line flow constraints, before and after the compensation) are used to examine the impact of SSSC and TCSC on total system social welfare improvement versus their cost. To validate the accuracy of the proposed method, several case studies are presented and simulation results are compared with those generated by genetic and Sequential Quadratic Programming (SQP) approaches.

1. Introduction

Competition in a deregulated power system will set a fair and equitable market structure and motivate all participants to maximize their own individual profits [1,2]. This will allow the market to behave in a manner that maximizes profit for all participants. In addition to deregulation challenges, electrical loads are rapidly growing, and some transmission lines are reaching their thermal limits.

Recently, much research has been done to improve the performance of transmission lines. Transmission expansion planning models, with their solutions, are organized in [3]. Similarly, several studies have been published in competitive electricity markets, based on transmission expansion. Optimal transmission network expansion; centralized and decentralized, is offered in [4]. A new market based transmission expansion planning is accessible in [5].

In conventional literature, transmission improvement methods are applied to achieve minimum generation costs, subject to system security constraints. In contrast, social welfare maximizing is the objective of most papers in deregulated power systems. Distributed generator locations for social welfare maximization are presented in [6]. Maximized social welfare is represented as the marginal benefit versus demand function in [7]. This reference discovered a method for increasing social welfare under congestion probability in transmission networks.

However, relieving congestion by building new transmission lines is an expensive solution that requires years for approval and construction. Different approaches have been proposed for optimal location of FACTS devices in both vertically integrated and unbundled power systems [8–15]. Recently, Flexible AC Transmission Systems (FACTS) have also been utilized to solve the congestion problem and maximize social welfare [9].

* Corresponding author.
E-mail addresses: h_nabavi@iust.ac.ir (S.M.H. Nabavi), kazemi@iust.ac.ir (A. Kazemi), m.masoum@curtin.edu.au (M.A.S. Masoum).

Peer review under responsibility of Sharif University of Technology.

Production and hosting by Elsevier

1026-3098 © 2012 Sharif University of Technology. Production and hosting by Elsevier B.V. All rights reserved.
doi:10.1016/j.scient.2011.04.028

Nomenclature

V_x, V_x^*, Z_x: Voltage, conjugated voltage and impedance
r_x, x_x, y_x: Resistance, reactance and admittance
P_x, Q_x, S_x: Active, reactive, and complex powers
$C(x)$, FF, F_x: Cost, fitness and penalty functions
N_x, R_x: Number of parameter x, random number

Subscripts

G, D, L: Generator, demand and line
i, it: Bus and iteration number

Superscripts

max, min: Maximum and minimum limits.

Sensitivity-based congestion management, with optimally placed FACTS controllers, is presented in [11,12]. Congestion management, using an Interline Power Flow Controller (IPFC), is performed in [12]. Application of a series of FACTS for congestion management in deregulated electricity markets is discussed in [13–15].

These references simplify the optimization problem by assuming given sizes of FACTS devices and/or the employment of second order generations cost functions, without considering sine components, due to valve point loading effects, and omitting load benefit functions in the objective function. In addition, the economic evaluation of SSSC and TCSC impact on social welfare has not been well addressed.

This paper proposes a Fuzzy-based Genetic Algorithm (Fuzzy-GA) for maximizing social benefit and alleviating congestion in a double-sided auction market by optimal location and sizing of Thyristor-Controlled Series Capacitor (TCSC) and Static Synchronous Series Compensator (SSSC) devices, considering their investment cost versus their economical benefits to power systems. Simulations are performed to investigate the impact of SSSC and TCSC on social welfare improvement, as opposed to their cost, on the modified IEEE 14-bus and 30-bus test systems, with quadratic smooth and quadratic nonsmooth (with sine components due to valve point loading effect) generator cost curves and quadratic smooth benefit functions for loads. The proposed method shows the benefits of SSSC and TCSC in a deregulated power market, and demonstrates how they may be utilized by ISO to improve total system social welfare and prevent congestion.

2. Mathematical model of TCSC and SSSC

Integration of FACTS devices in load flow analysis and issues related to Optimal Power Flow (OPF) in the context of a pool paradigm, has been reported in [13,15]. In this paper, the Newton–Raphson (N–R) power flow formulation is used, and TCSC and SSSC are represented using a Power Injection Model (PIM) [13–16]. This will allow easy integration of FACTS devices into the existing power system software tools, and retain the symmetrical structure of the admittance matrix. In the PIM model (Figure 1(a)), changes in the line flow, due to FACTS devices, are represented as a line without these devices with powers injected at receiving and sending ends.

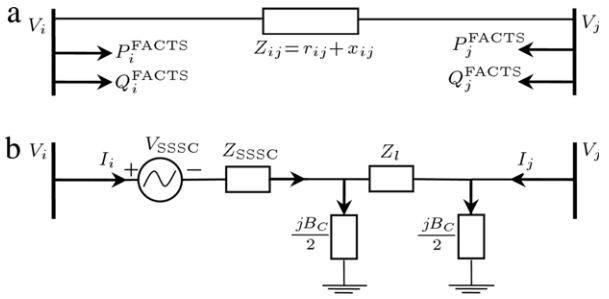

Figure 1: (a) Power injection model of a transmission line with FACTS devices. (b) Equivalent circuit of the embedded SSSC.

2.1. Power injection model of TCSC and SSSC

With a TCSC unit connected in line ij, the injected real and reactive power at buses i and j are as follows [13–15]:

$$P_i^{\text{TCSC}} = V_i^2 \Delta G_{ij} - V_i V_j [\Delta G_{ij} \cos\delta_{ij} + \Delta B_{ij} \sin\delta_{ij}], \quad (1)$$

$$P_j^{\text{TCSC}} = V_j^2 \Delta G_{ij} - V_i V_j [\Delta G_{ij} \cos\delta_{ij} - \Delta B_{ij} \sin\delta_{ij}], \quad (2)$$

$$Q_i^{\text{TCSC}} = -V_i^2 \Delta B_{ij} - V_i V_j [\Delta G_{ij} \sin\delta_{ij} - \Delta B_{ij} \cos\delta_{ij}], \quad (3)$$

$$Q_i^{\text{TCSC}} = -V_j^2 \Delta B_{ij} + V_i V_j [\Delta G_{ij} \sin\delta_{ij} + \Delta B_{ij} \cos\delta_{ij}], \quad (4)$$

where

$$\Delta G_{ij} = x_c r_{ij}(x_c - 2x_{ij})/(r_{ij}^2 + x_{ij}^2)(r_{ij}^2 + (x_{ij} - x_c)^2)$$

and

$$\Delta B_{ij} = -x_c(r_{ij}^2 - x_{ij}^2 + x_c x_{ij})/(r_{ij}^2 + x_{ij}^2)(r_{ij}^2 + (x_{ij} - x_c)^2).$$

Also, by using SSSC (Figure 1(b)), the real and reactive power injections at bus i (P_i^{SSSC}, Q_i^{SSSC}) and bus j (P_j^{SSSC}, Q_j^{SSSC}) can be expressed as [16]:

$$P_i^{\text{SSSC}} = V_i V_{\text{SSSC}} (1 - B_C X_l/2) \sin(\theta_i - \theta_{\text{SSSC}})/H, \quad (5)$$

$$Q_i^{\text{SSSC}} = -V_i V_{\text{SSSC}} (1 - B_C X_l/2) \cos(\theta_i - \theta_{\text{SSSC}})/H, \quad (6)$$

$$P_j^{\text{SSSC}} = -V_j V_{\text{SSSC}} \sin(\theta_j - \theta_{\text{SSSC}})/H, \quad (7)$$

$$Q_j^{\text{SSSC}} = V_j V_{\text{SSSC}} \cos(\theta_j - \theta_{\text{SSSC}})/H, \quad (8)$$

where $H = X_{\text{SSSC}} - B_C X_{\text{SSSC}} X_l/2 + X_l$.

Due to the fact that SSSC neither absorbs nor injects real power, with respect to the AC system, the real power exchange via the DC link is zero:

$$\begin{aligned} P_{\text{ex}} &= \text{Re}(V_{\text{SSSC}} I_i^*) \\ &= (B_C - X_l B_C^2/4 + G/H) V_{\text{SSSC}} V_j \sin(\theta_{\text{SSSC}} - \theta_j) \\ &\quad - (1 - B_C X_l/2) V_{\text{SSSC}} V_i \sin(\theta_{\text{SSSC}} - \theta_j)/H = 0, \end{aligned} \quad (9)$$

where:

$$G = [-X_{\text{SSSC}}(B_C - X_l B_C^2/4) + 1 - X_l B_C/2](1 - X_l B_C/2).$$

The resistances of transmission lines and the coupling transformer of SSSC are neglected. Eqs. (1)–(9) are added to the Jacobian matrix in N–R load flow formulations.

2.2. Cost of TCSC and SSSC

In this paper, the cost of TCSC is included using the following linear equation [15]:

$$\text{Cost(TCSC)} = C x_{c,k} \frac{S_{\max}^2}{S_B}, \quad (10)$$

where $C = 22{,}000$ \$/MVA-year is the cost coefficient of TCSC, $S_{\max}$ (in MVA) is the thermal limit of the line, where the kth TCSC device is placed, S_B is the base MVA power, and $x_{c,k}$ is the kth series capacitive reactance (pu). In this paper, the cost of a SSSC is assumed the same as [17]. According to the above formulation, the cost of TCSC depends on its capacity.

3. Problem formulation

3.1. Objective function

In this paper, a double action pool market is used to dispatch generation and load in an economic manner. In the double auction pool market model, both DisCos and GenCos participate in the market, and offer their bid-quantity packages to the market operator. The objective of a market operator is to maximize social welfare including load flow equality and operational inequality constraints as follows:

$$\text{Max}\left(\sum_{j=1}^{N_D}(a_{dj}+b_{dj}P_{Dj}+c_{dj}P_{Dj}^2)-\sum_{i=1}^{N_G}(a_{gi}+b_{gi}P_{Gi}+c_{gi}P_{Gi}^2)-\left|e_{gi}\times\text{Sin}(f_{gi}\times(P_{Gi}-P_{\text{mini}}))\right|-\text{FACTS}_{\text{Cost}}\right). \quad (11)$$

The components of Eq. (11) include:

- *The DisCos benefit functions* are assumed to be quadratic:

$$B(P_D)=\sum_{j=1}^{N_D}(a_{dj}+b_{dj}P_{Dj}+c_{dj}P_{Dj}^2), \quad (12)$$

where P_{Dj} is dispatched load at nodes j, N_D is the number of loads, and "a_{dj}, b_{dj}, c_{dj}" are benefit function coefficients. Inclusion of Eq. (12) in the objective function of the OPF problem will guarantee that Locational Marginal Prices (LMPs) charged at the demand buses are less than, or equal to, the DisCos benefit, earned by selling that power to retail customers. In case of congestion in the system, the OPF will give a signal to reduce the demand by a particular amount at those buses for which marginal benefit is less than marginal price, ultimately leading to a reduction in system congestion [18].
- *The overall generation cost functions* are modeled by smooth quadratic (convex and differentiable) functions:

$$C(P_G)=\sum_{i=1}^{N_G}(a_{gi}+b_{gi}P_{Gi}+c_{gi}P_{Gi}^2). \quad (13)$$

These functions are used to set the generators on the best operation point to minimize total system generation cost, considering all network constraints. To include the valve point loading effect in Eq. (13), an additional sine term is included as follows:

$$C(P_G)=\left\{\sum_{i=1}^{N_G}(a_{gi}+b_{gi}P_{Gi}+c_{gi}P_{Gi}^2)+\left|e_{gi}\times\text{Sin}(f_{gi}\times(P_{Gi}-P_{\text{mini}}))\right|\right\}. \quad (14)$$

It is obvious that considering valve point loading changes the operation point for the generators, and their generation cost. This more accurate modeling adds more challenges to most derivative-based optimization algorithms in finding a global solution, since the objective is no longer convex or differentiable everywhere.

- *The FACTS devices cost function* will be included using Eq. (10). In this paper, the investment cost of TCSC and SSSC devices are used to illustrate their impact on social welfare maximizing against their costs.

3.2. Constraints

The objective function (Eq. (11)) is subjected to the following constraints:

(i) *Power injection*: at each bus, the total injected active and reactive power should be zero:

$$P_i(\theta,V)-P_{Gi}+P_{Di}+P_i^{\text{FACTS}}=0, \quad (15)$$

$$Q_i(\theta,V)-Q_{Gi}+Q_{Di}+Q_i^{\text{FACTS}}=0, \quad (16)$$

$$P_j(\theta,V)-P_{Gj}+P_{Dj}+P_j^{\text{FACTS}}=0, \quad (17)$$

$$Q_j(\theta,V)-Q_{Gj}+Q_{Dj}+Q_j^{\text{FACTS}}=0. \quad (18)$$

(ii) *Generation limits*: the upper and lower limits of generator outputs are considered as:

$$P_{Gi}^{\min}\le P_{Gi}\le P_{Gi}^{\max}\quad \text{for } i=1,\ldots,N_G, \quad (19)$$

$$Q_{Gi}^{\min}\le Q_{Gi}\le Q_{Gi}^{\max}\quad \text{for } i=1,\ldots,N_G, \quad (20)$$

where P_{Gi} and Q_{Gi} are the active and reactive power generation vectors at bus G_i, respectively.

(iii) *Demand limits*: the maximum and minimum limits of consumer demands are considered as:

$$P_{Dj}^{\min}\le P_{Dj}\le P_{Dj}^{\max}\quad \text{for } j=1,\ldots,N_D, \quad (21)$$

$$Q_{Dj}^{\min}\le Q_{Dj}\le Q_{Dj}^{\max}\quad \text{for } j=1,\ldots,N_D, \quad (22)$$

where P_{Dj} and Q_{Dj} are the active and reactive power demand vectors at bus D_j, respectively.

(iv) *Transmission constraints*: the MVA limit of the transmission line is included as:

$$|S_l(\theta,V)|^2\le(S_l^{\max})^2, \quad (23)$$

where transmission flows are:

$$P_{ij}(\theta,V)=\text{Re}\left[V_i^*(V_i-V_j)y_{ij}+V_i^*V_iy_{i_0}\right], \quad (24)$$

$$Q_{ij}(\theta,V)=-\text{Im}\left[V_i^*(V_i-V_j)y_{ij}+V_i^*V_iy_{i_0}\right], \quad (25)$$

$$S_{ij}(\theta,V)=V_i^*(V_i-V_j)y_{ij}+V_i^*V_iy_{i_0}, \quad (26)$$

$$P_{ji}(\theta,V)=\text{Re}\left[V_j^*(V_j-V_i)y_{ij}+V_j^*V_jy_{j_0}\right], \quad (27)$$

$$Q_{ji}(\theta,V)=-\text{Im}\left[V_j^*(V_j-V_i)y_{ij}+V_j^*V_jy_{ij_0}\right], \quad (28)$$

$$S_{ji}(\theta,V)=V_j^*(V_j-V_i)y_{ij}+V_j^*V_jy_{j_0}, \quad (29)$$

$$S_l(\theta,V)=\text{Max}(S_{ij},S_{ji}). \quad (30)$$

y_{i_0} and y_{j_0} are the line charging admittances and y_{ij} is the admittance of the transmission line between nodes i and j.

Eq. (23) ensures that no congestion occurs in transmission lines in the procedure of double action market clearing.

(v) *Voltage limits*: the minimum and maximum voltage levels at each bus are included as:

$$V_i^{\min}\le V_i\le V_i^{\max}. \quad (31)$$

(vi) *Compensation limit*: the upper and lower compensation levels of equivalent TCSC reactance (x_c) are included as:

$$x_c^{\min}\le x_c\le x_c^{\max}. \quad (32)$$

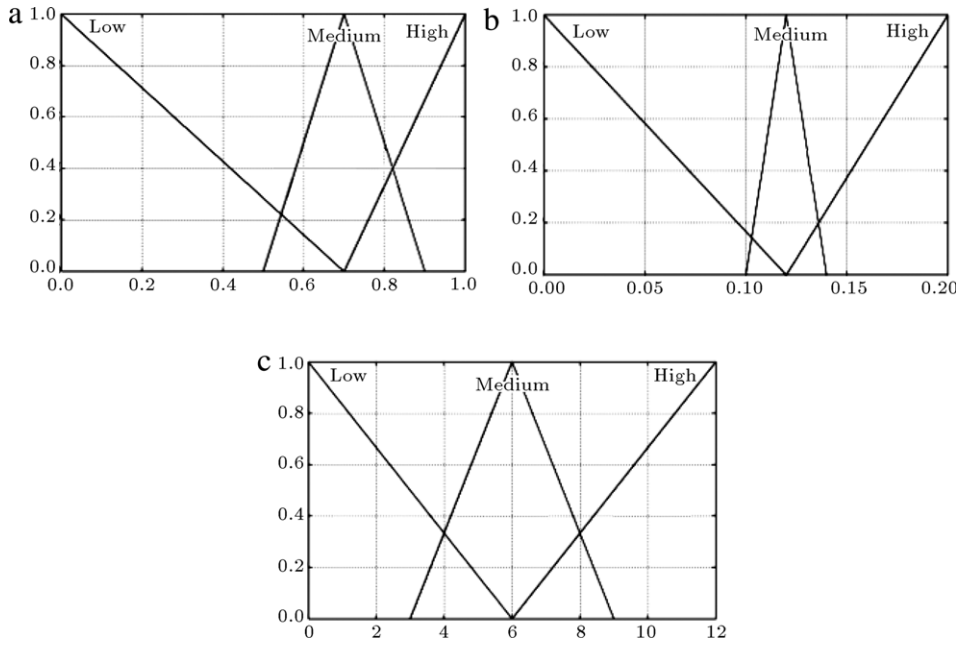

Figure 2: Proposed membership functions. (a) *BF* (best fitness for each generation); (b) *VF* (variance of fitness values of objective function); and (c) *UN* (number of generations with no significant impact on *BF*).

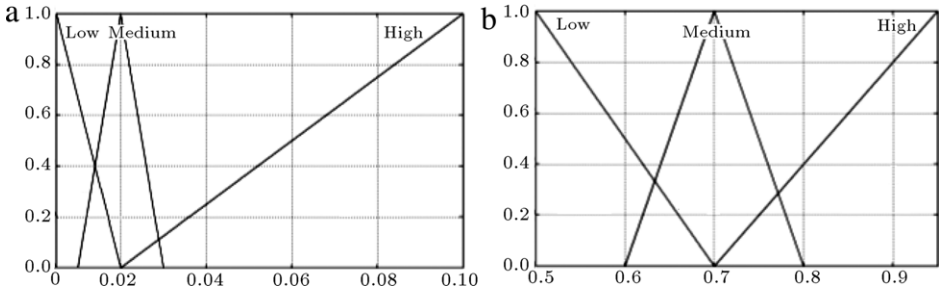

Figure 3: Membership function and range of output variables. (a) Probability of mutation *Pm*; and (b) probability of crossover *Pc*.

(vi) *Compensation limit*: the maximum and minimum values of SSSC voltage (V_{Se}) and its angle (θ_{Se}) are included as:

$$V_{Se}^{\min} \leq V_{Se} \leq V_{Se}^{\max}, \tag{33}$$

$$\theta_{Se}^{\min} \leq \theta_{Se} \leq \theta_{Se}^{\max}. \tag{34}$$

4. Proposed fuzzy-genetic algorithm

The Genetic Algorithm (GA) is a global search technique, based on the mechanisms of natural selection and genetics, capable of searching several possible solutions simultaneously [19,20]. GA has been applied to many problems including stability studies, load frequency control, unit commitment, reactive power compensation and V/Q/THD control [21,22].

4.1. The proposed fuzzy-GA method

The optimization problem of Eq. (11) is a complex *large-scale nonlinear* programming dilemma that cannot easily be solved by conventional approaches. This paper proposes a Fuzzy-GA approach to capture the best solution of Eq. (11). The GA performance is improved by dynamically changing the probabilities of crossover (*Pc*) and mutation (*Pm*), according to a fuzzy knowledge base (Figures 2–5) that has been developed

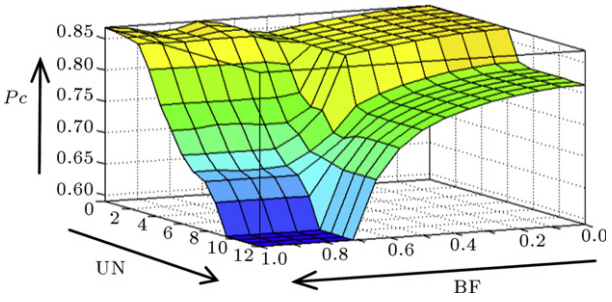

Figure 4: Variations of crossover (*Pc*) imposed by the fuzzy rules.

from experience [23]. Variations of *Pc* and *Pm* have been divided into LOW, MEDIUM and HIGH membership functions, with given membership values as shown in Figures 2 and 3. Incorporation of fuzzy logic in GA will improve performance and reduce search time.

In order to determine fitness function values, GA parameters (*Pc* and *Pm*) are varied, based on the following logic:

- The value of best fitness for each generation (*BF*) is expected to change with the number of generations. However, if *BF* does not change significantly over a number of generations (*UN*), then this information is considered to make changes in both *Pc* and *Pm*.

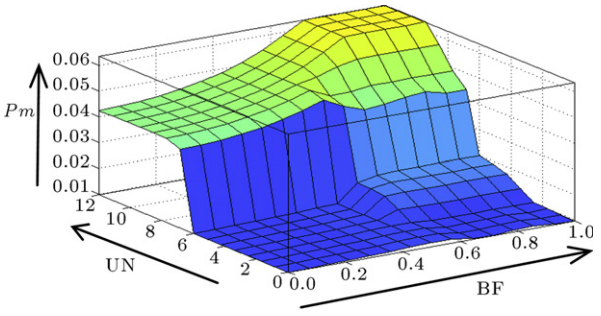

Figure 5: Variations of mutation (Pm) imposed by the fuzzy rules.

Table 1: Fuzzy rules incorporated in GA to improve the probabilities of mutation (Pm) and crossover (Pc).

Rule #	*BF*	*UN*	*VF*	*Pc*	*Pm*
1	Low	None	None	High	Low
2	Medium	Low	None	High	Low
3	Medium	Medium	None	Medium	Medium
4	High	Low	None	High	Low
5	High	Medium	None	Medium	Medium
6	None	High	Low	Low	High
7	None	High	Medium	Low	High
8	None	High	High	High	Low

- The diversity of a population influences the search for a true optimum. Therefore, variance of the fitness values (*VF*) is considered to also have impact on *Pc* and *Pm*.
- The membership functions and membership values for *BF*, *UN* and *VF* are selected after several trials to ensure optimum results (Figures 2 and 3).

4.2. Proposed fuzzy rules

Eight fuzzy rules are used to adjust mutation and crossover rates, as shown in Table 1 [23]. Variations of crossover and mutation are also plotted in Figures 4 and 5. Note that *Pc* starts at 0.9, with an exponential variation. As the algorithm approaches the optimal solution, *Pc* will be reduced and *Pm* will be bounded between 0 and 0.1.

5. Development of the fuzzy-GA approach

The optimization problem consists of solving Eq. (11), with incorporation of SSSC and TCSC devices, for social welfare maximization on pool market based power systems.

5.1. Initial population and structure of chromosomes

To begin the GA, a random number generator is used to select the initial population chromosomes within the range of the control variables. In this paper, the selected chromosome structure contains generation and demand levels, as well as TCSC location and compensation level, or SSSC location and compensation parameters (Figure 6). The randomly generated chromosomes are used in real code to provide higher accuracy as compared with binary coding.

5.2. Proposed fitness function

GA procedure involves the evaluation of objective (fitness) functions to measure the quality of the solutions. A solution with a better quality (e.g., higher fitness value) will be included in the new population, while low quality solutions are discarded. In this paper, exponential penalty functions for each generated chromosome are calculated for lines that have power overflows and/or reach voltage, generation and load limits based on respective penalty functions as follows:

$$F_{\text{Fitness}} = F_{\text{Line flow}} \times F_{\text{Busvoltage}} \times F_{\text{Generation}} \times F_{\text{Load}} \times F_{\text{Reactive Gen}} \times F_{\text{Reactive Dem}}, \tag{35}$$

$$F_{\text{Line flow}} = \prod_{j=1}^{N_L} F_L, \tag{36}$$

$$F_{\text{Bus voltage}} = \prod_{j=1}^{N_B} F_V, \tag{37}$$

$$F_{\text{Generation}} = \prod_{j=1}^{N_G} F_G, \tag{38}$$

$$F_{\text{Reactive Gen}} = \prod_{j=1}^{N_G} F_{QG}, \tag{39}$$

$$F_{\text{Reactive Dem}} = \prod_{j=1}^{N_D} F_{QD}, \tag{40}$$

$$F_{\text{Load}} = \prod_{j=1}^{N_D} F_D, \tag{41}$$

where N_L, N_G, N_D and N_B are the number of branches, generators, loads and buses in the power system, respectively, and F_{fitness} is the fitness function value for each chromosome. The proposed penalty functions are:

$$F_L = \begin{cases} 1 & \text{line flow} < \text{line flow}_{\text{Max}} \\ e^{\alpha_I(\text{line flow}_{\text{Max}} - \text{line flow})} & \text{line flow} > \text{line flow}_{\text{Max}} \end{cases} \tag{42}$$

$$F_G = \begin{cases} e^{-\alpha_{G1}(P_{\text{generation}})} - 1 & P_{\text{generation}} < P_{\text{generation\_Min}} \\ 1 & P_{\text{generation\_Min}} \le P_{\text{generation}} \le P_{\text{generation\_Max}} \\ e^{\alpha_{G2}(P_{\text{generation}_{\text{Max}}} - P_{\text{generation}})} & P_{\text{generation}} > P_{\text{generation\_Max}} \end{cases} \tag{43}$$

$$F_V = \begin{cases} e^{-\alpha_{V1}(V_{\text{Bus}})} - 1 & V_{\text{Bus}} < V_{\text{Min}} \\ 1 & V_{\text{Min}} \le V_{\text{Bus}} \le V_{\text{Max}} \\ e^{-\alpha_{V2}(V_{\text{Max}} - V_{\text{Bus}})} & V_{\text{Bus}} > V_{\text{Max}} \end{cases} \tag{44}$$

$$F_D = \begin{cases} e^{-\alpha_{L1}(P_{\text{Load}})} - 1 & P_{\text{Load}} < P_{\text{Load Min}} \\ 1 & P_{\text{Load Min}} \le P_{\text{Load}} \le P_{\text{Load Max}} \\ e^{-\alpha_{L2}(P_{\text{Load}_{\text{Max}}} - P_{\text{Load}})} & P_{\text{Load}} > P_{\text{Load Max}} \end{cases} \tag{45}$$

$$F_{QD} = \begin{cases} e^{-\alpha_{QD1}(Q_{\text{Load}})} - 1 & Q_{\text{Load}} < Q_{\text{Load Min}} \\ 1 & Q_{\text{Load Min}} \le Q_{\text{Load}} \le Q_{\text{Load Max}} \\ e^{-\alpha_{QD2}(Q_{\text{Load}_{\text{Max}}} - Q_{\text{Load}})} & Q_{\text{Load}} > Q_{\text{Load Max}} \end{cases} \tag{46}$$

$$F_{QG} = \begin{cases} e^{-\alpha_{QG1}(Q_{\text{generation}})} - 1 & Q_{\text{generation}} < Q_{\text{generation\_Min}} \\ 1 & Q_{\text{generation\_Min}} \le Q_{\text{generation}} \le Q_{\text{generation\_Max}} \\ e^{\alpha_{QG2}(Q_{\text{generation}_{\text{Max}}} - Q_{\text{generation}})} & Q_{\text{generation}} > Q_{\text{generation\_Max}} \end{cases} \tag{47}$$

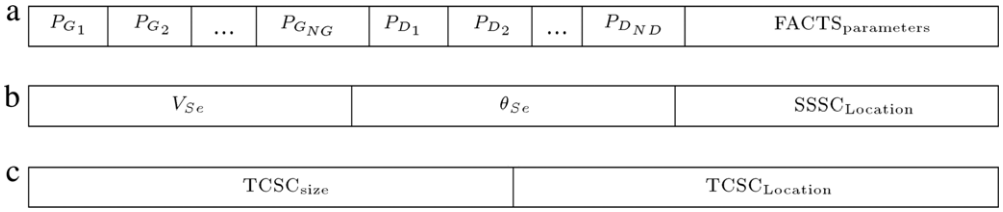

Figure 6: (a) Chromosome structure for the GA; (b) SSSC parameters and location; and (c) TCSC size and location.

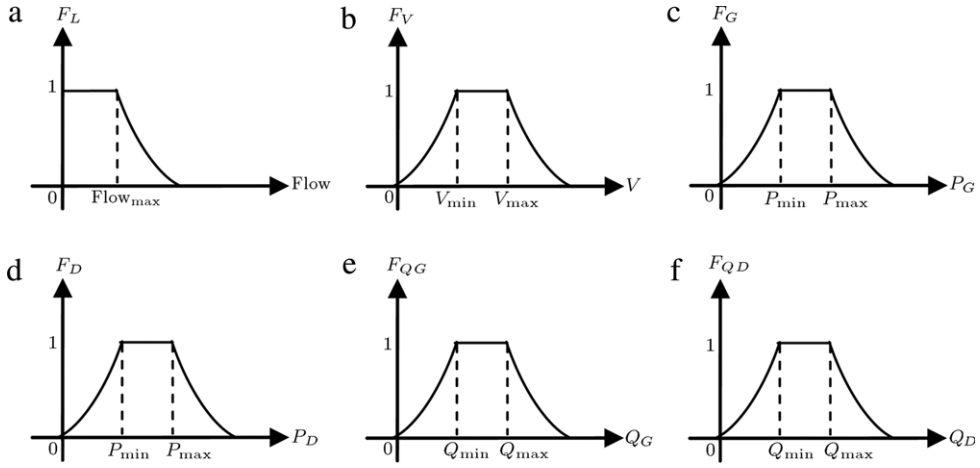

Figure 7: Penalty functions used to compute fitness (Eq. (9)). (a) F_L; (b) F_V; (c) F_G; (d) F_D; (e) F_{QG}; and (f) F_{QD}.

where $\alpha_I, \alpha_{G1}, \alpha_{G2}, \alpha_{L1}, \alpha_{L2}, \alpha_{V1}$ and α_{V2} are the coefficients used to adjust the slope of penalty functions (Figure 7).

5.3. Genetic operators

Genetic operators are the stochastic transition rules applied to each chromosome during each generation procedure to create a new improved population from an old one.

- *Reproduction* is a probabilistic process for selecting two parent strings from the population of strings. In this paper, two reproduction methods, including; *tournament* and *roulette wheel*, have been tested and compared. Tournament selection has several benefits: it is more efficient to code, works on parallel architectures and allows the selection pressure to be easily adjusted. It was observed that this method is faster, more stable and exhibits better convergence.
- *Crossover* is to recombine blocks on different individuals to make a new one. In this paper, Heuristic crossover is used to generate a single offspring variable, p_{new}, from a combination of two corresponding offspring values:

$$p_{\text{new}} = \beta(p_{mn} - p_{dn}) + p_{mn}, \tag{48}$$

- where β is a random number on the interval $(0, 1)$, p_{mn} and p_{dn} are the nth variables in the parent chromosomes. The probability of crossover is selected by the proposed fuzzy rules (Figure 4) to be between 0.5 and 0.95.
- *Mutation* introduces artificial diversification in the population to prevent complete loss of data through reproduction and crossover, by ensuring that the probability of searching any region in the problem space is never zero. In this paper, dynamic (or nonuniform) mutation is implemented for fine-tuning and achieving a high degree of precision. For a given parent, x, the resulting gene is selected from:

$$x'_k = x_k \times \left\{1 + (-1)^t \times \left[1 - r^{\left(1-\frac{t}{T}\right)^b}\right]\right\}, \tag{49}$$

where r is a uniform random number on interval $(0, 1)$, t is the current generation number, T is the maximum number of generations and b (e.g., $b = 2$ in this paper) is a parameter determining the impact of mutation on the new generations. The probability of mutation is selected by fuzzy rules (Figure 5) to be between 0 and 0.1.

5.4. Population replacement

Two population replacement methods, non-overlapping generations and steady-state replacement, are used. When using non-overlapping generations (e.g., replacing the entire generation by its offspring), it is possible for offspring to be worse than their parents, and some fitter chromosomes may be lost from the evolutionary process. Steady-state replacement (e.g., creating a number of offspring to replace the least fit individuals) overcomes this problem and was found to provide better convergence criteria.

5.5. Convergence criterion

The iterations (regenerations) are continued until all generated chromosomes become equal, or the maximum number of iterations is achieved ($N^{\max} = 1000$). Due to the randomness of the GA method, the solution tends to differ for each run, even with the same initial population. It is suggested to perform multiple runs and select the "most acceptable" solution.

6. Solution methodology

The problem defined by Eqs. (11)–(34) is solved using the proposed Fuzzy-GA of Figure 8. The main steps are as follows:

Step 1: Input power system parameters, including system configuration, line parameters, load data, generator constraints, line flow limits and load/generator cost coefficients.

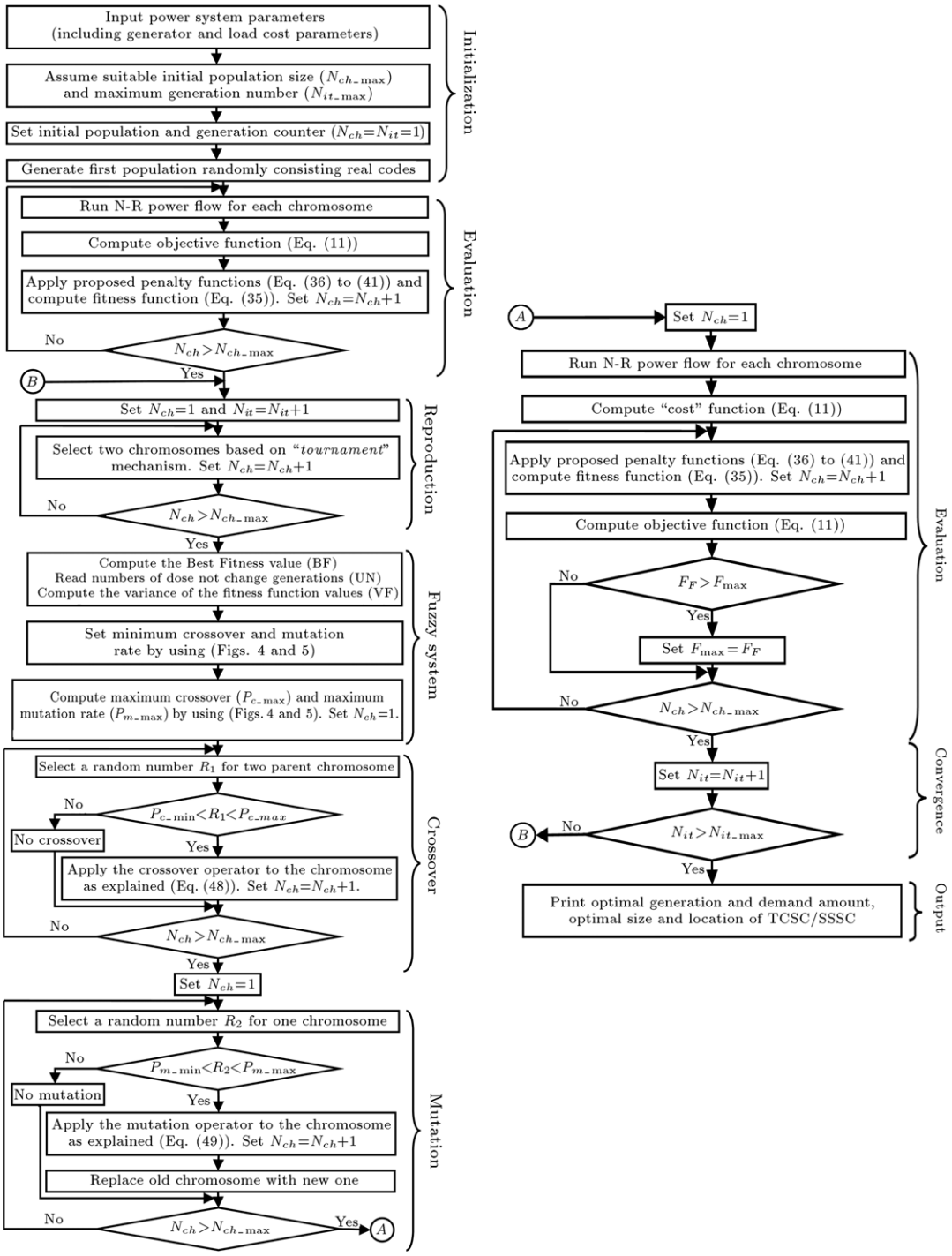

Figure 8: Proposed Fuzzy-GA algorithm for social welfare maximization by optimal location and sizing of TCSC/SSSC.

Step 2: Assume a suitable population size (N_{ch_max}) and maximum number of generations (N_{it_max}). Set initial counters and parameter values (e.g., $N_{ch} = N_{it} = 1$), and generate random chromosomes by real coding.

Step 3 (Fitness Process):

Step 3A: Run power flow for each set of chromosomes, calculate the voltage (magnitude and phase angle) at each bus and determine the power flow for each transmission line.

Step 3B: Compute proposed penalty functions (Figure 7) using outputs of the applied power flow. Compute fitness functions (Eq. (31)) for chromosome N_{ch}, and set $N_{ch} = N_{ch} + 1$.

Step 3C: If $N_{ch} \leq N_{ch\_max}$, go to Step 3A.

Step 4 (Reproduction Process):

Step 4A: Define total fitness as the product of all fitness values for all chromosomes.

Step 4B: Run a *tournament* for the selection process. Select a new combination of chromosomes.

Step 5 (Crossover Process):

Step 5A: Compute the cross over probability by using the proposed fuzzy rules (Figure 4).
Step 5B: Select a random number (R_1) for mating two parent chromosomes.
Step 5C: If R_1 is between the computed maximum and minimum values of crossover, then, combine the two parents, generate two offspring, and go to Step 5E.
Step 5D: Else, transfer the chromosome with no crossover.
Step 5E: Repeat steps 5A to 5D for all chromosomes.

Step 6 (Mutation Process):

Step 6A: Compute the mutation probability by using the proposed fuzzy rules (Figure 5).
Step 6B: Select a random number (R_2) for mutation of one chromosome.
Step 6C: If R_2 is between the computed maximum and minimum values of mutation, then, apply the mutation process and go to Step 6E.
Step 6D: Else, transfer the chromosome with no mutation.
Step 6E: Repeat Steps 6A to 6C for all chromosomes.

Step 7 (Updating Populations): Replace the old population with the improved population generated by Steps 2–6. Check all chromosomes. If there is any chromosome with $F_L = 1, F_G = 1, F_V = 1, F_D = 1, F_{QG} = 1, F_{QD} = 1$ and $F_F > F_{\max}$, set $F_{\max} = F_F$ and save it. Set $N_{it} = N_{it} + 1$.

Step 8 (Convergence): If the maximum number of iterations is achieved, then, print the solution and stop, else, go to Step 3.

7. Simulation cases

This section presents the basic operation of the modified IEEE 14-bus (Figure 9) [15] and Table A.1 and the modified IEEE 30-bus (Figure 10) [24] and Table A.2 test systems, as well as the location and sizing of TCSC/SSSC units with smooth/nonsmooth generator cost curves (Eq. (10)) without/with transmission line flow constraints (Eqs. (13)–(15)). In the modified IEEE 14-bus test system, the objective function consists of 13 variables for 5-generation nodes (G5 only generates reactive power) and 8-demand nodes. Similarly, in the modified IEEE 30-bus test system, the objective function consists of 30 variables for 9-generation nodes and 21-demand nodes.

In addition, 2 variables for TCSC parameters and 3 SSSC parameters are added to the variables of the objective function in each test system. There are 20 and 41 possible locations to place TCSC/SSSC units in the modified IEEE 14-bus and modified IEEE 30-bus test systems, respectively.

In this paper, the minimum and maximum series capacitive compensation levels of TCSC are limited to 0% and 70% of the compensated line reactance, respectively. In addition, it is assumed that the SSSC reactance is 0.05 pu, maximum SSSC voltage is 0.1 pu and its angle can change from 0° to 180°.

Figure 11 shows the highly convex shape of the fuel cost function of two-generation units when the valve point effects are included. Note that, even when considering only two units, there are multiple peaks and differentiable valleys [19]. Therefore, the optimization problem, with addition of the sine components, has become too complex to be solved using gradient-based approaches.

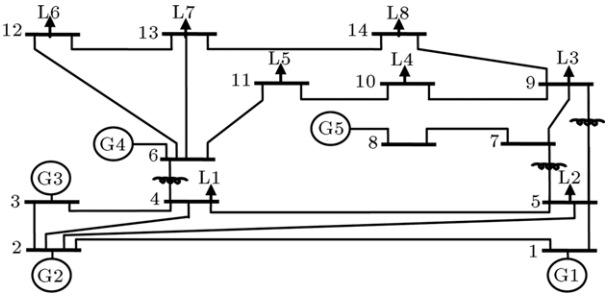

Figure 9: The modified IEEE 14-bus test system.

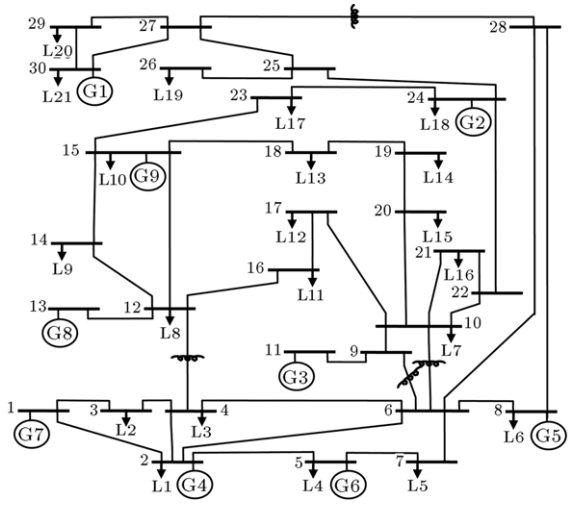

Figure 10: The modified IEEE 30-bus test system.

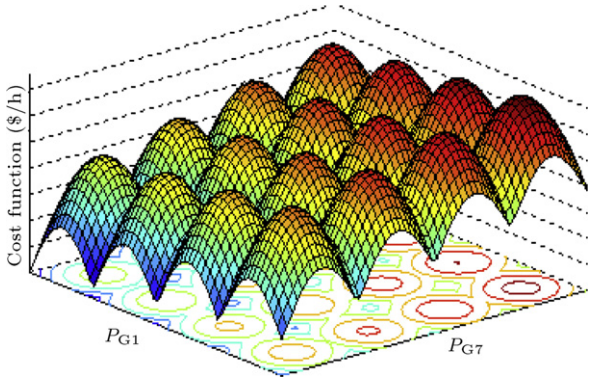

Figure 11: High degree of convexity in the shape of the objective fuel cost function of two-generation units including valve-loading effects [19].

According to Table 2, forty cases are studied to demonstrate the ability of the proposed Fuzzy-GA method (Figure 8) as follows:

Cases A1 and A2: Base operation of the modified IEEE 14-bus test system without line flow constraints and without FACTS, using smooth and nonsmooth generation cost functions, respectively.

Cases A3 and A4: Base operation of the modified IEEE 14-bus test system with line flow constraints and without FACTS, using smooth and nonsmooth generation cost functions, respectively.

Cases A5 and A6: Base operation of the modified IEEE 14-bus test system with line flow constraints and with TCSC, using smooth and nonsmooth generation cost functions, respectively.

Table 2: Simulated cases of the IEEE 14-bus and IEEE 30-bus systems.

Test system		Simulated cases	Results
IEEE 14-bus (Figure 9)	A	Base operation without/with SSSC	Tables 3–5, 7–10 and Figure 12
IEEE 30-bus (Figure 10)	B	Base operation without/with SSSC	Tables 3–4 and 6–10
	C	Outage of line 2–4 (between buses 2 and 4)	
	D	Outage of unit 4 at bus 2	
	E	Increase of load 3 (by 150%) at bus 4	

Table 3: Cost-benefit analysis by the proposed Fuzzy-GA for the modified IEEE 14-bus and IEEE 30-bus systems with smooth and nonsmooth cost curves.

Generator	Smooth generation cost curve						Nonsmooth generation cost curve			
	Proposed method				SQP [25]		Proposed method			
	Without line flow constraints and without FACTS	With line flow constraints and without FACTS	With line flow constraints and with TCSC	With line flow constraints and with SSSC	Without line flow constraints and without FACTS	With line flow constraints and without FACTS	Without line flow constraints and without FACTS	With line flow constraints and without FACTS	With line flow constraints and with TCSC	With line flow constraints and with SSSC
G1	94.22	97.25	88.84	90.17	100	88.15	90.08	90.64	88.84	90.17
G2	100	100	100	100	100	100	100	100	100	100
G3	100	100	100	100	100	100	100	100	100	100
G4	92.83	48.9	63.59	60.96	92.38	62.88	91.83	46.26	63.59	60.962
L1	58.10	116.90	107.7	108.7	58.10	116.90	55.15	121.01	107.7	108.72
L2	55.63	125.14	116.2	99.778	55.63	125.14	52.49	112.86	116.2	99.778
L3	5.63	8.02	5	12.731	5.63	8.02	5.02	5.94	5	12.731
L4	21.54	16.86	26.8	15.844	21.54	16.86	29.73	16.08	26.8	15.8441
L5	35.79	22.15	15.4	27.388	35.79	22.15	26.32	23.97	15.4	27.389
L6	51.88	31.23	25.9	45.763	51.88	31.23	54.10	30.18	25.9	45.764
L7	71.90	7.16	9.2	17.672	71.90	7.16	71.49	6.68	9.2	17.672
L8	62.33	7.604	29.5	11.2973	62.33	7.604	63.45	10.88	29.5	11.297

Cases A7 and A8: Base operation of the modified IEEE 14-bus test system with line flow constraints and with SSSC, using and nonsmooth generation cost functions, respectively.

Cases B1 and B2: Base operation of the modified IEEE 30-bus test system without line flow constraints and without FACTS, using smooth and nonsmooth generation cost functions, respectively.

Case B3 and B4: Base operation of the modified IEEE 30-bus test system with line flow constraints and without FACTS, using smooth and nonsmooth generation cost functions, respectively.

Case B5 and B6: Base operation of the modified IEEE 30-bus test system with line flow constraints and with TCSC, using smooth and nonsmooth generation cost functions, respectively.

Case B7 and B8: Base operation of the modified IEEE 30-bus test system with line flow constraints and with SSSC, using smooth and nonsmooth generation cost functions, respectively.

Similarly, optimizations have been done for the modified IEEE 30-bus test system, considering unit or line outage and load increasing, for the other 24 cases (Cases C1–E8).

Selected parameters for the proposed optimization method are: number of generations = 1000, number of populations = 73, crossover rate = 0.5–0.95 (selected by the proposed fuzzy rules of Figure 4), and mutation rate = 0–0.1 (selected by the fuzzy rules of Figure 5). Note that, for the modified IEEE 30-bus test system, the second consumer benefit coefficient (b_d) is multiplied by 5 to increase the benefit function.

8. Simulation results

8.1. Algorithm validation

In this stage, 10 cases (A1, A3, B1, B3, C1, C3, D1, D3, E1 and E3) are studied to illustrate the ability of the proposed method. Tables 3 and 4 present comparisons of simulation results generated by the proposed Fuzzy-GA (Figure 8) and MATPOWER. MATPOWER is a toolbox that solves the OPF, using sequential quadratic programming with smooth objective functions [25].

In addition, according to column 9 in Table 3, it can be seen that there is a little difference (less than 1%) between SQP outcomes and the proposed fuzzy based genetic algorithm for social welfare. This difference is calculated, using:

$$\Delta SW(\%) = \frac{\left|SW_{\mathrm{FGA}} - SW_{\mathrm{SQP}}\right|}{SW_{\mathrm{FGA}}} \times 100. \tag{50}$$

It should be noted that there are slight differences in case A, due to differences in the amount of demand and generation using the SQP and the proposed method.

According to Table 4, it can be seen that by applying a sinusoidal part, the SQP based method is not accountable, while the proposed method can solve the optimization problem (Eq. (11)).

8.2. Operation without TCSC/SSSC

According to Table 5 (rows 12–15, columns 2 and 5), without any line flow constraints, there are very high load demands at nodes 11–14 (corresponding to loads 5–8), due to higher benefit coefficients (Eq. (12)). However, when the line flow constraints are considered (Table 5, rows 12–15, columns 3 and 6), there are substantial reductions in load demand and social benefit at theses nodes (Figure 12).

Line flow constraints will substantially increase loading levels (Table 5) at nodes 4–5 (corresponding to loads 1–2) and increase social benefits (Figure 12). It shows that loads 1–3, in spite of having lower profit coefficients than loads

Table 4: System analysis results for the modified IEEE 14-bus and IEEE 30-bus test systems (powers are in MW).

Generator	Smooth generation cost curve						Nonsmooth generation cost curve			
	Proposed method				SQP [25]		Proposed method			
	Without line flow constraints and without FACTS	With line flow constraints and without FACTS	With line flow constraints and with TCSC	With line flow constraints and with SSSC	Without line flow constraints and without FACTS	With line flow constraints and without FACTS	Without line flow constraints and without FACTS	With line flow constraints and without FACTS	With line flow constraints and with TCSC	With line flow constraints and with SSSC
G1	94.22	97.25	88.84	90.17	100	88.15	90.08	90.64	88.84	90.17
G2	100	100	100	100	100	100	100	100	100	100
G3	100	100	100	100	100	100	100	100	100	100
G4	92.83	48.9	63.59	60.96	92.38	62.88	91.83	46.26	63.59	60.962
L1	58.10	116.90	107.7	108.7	58.10	116.90	55.15	121.01	107.7	108.72
L2	55.63	125.14	116.2	99.778	55.63	125.14	52.49	112.86	116.2	99.778
L3	5.63	8.02	5	12.731	5.63	8.02	5.02	5.94	5	12.731
L4	21.54	16.86	26.8	15.844	21.54	16.86	29.73	16.08	26.8	15.8441
L5	35.79	22.15	15.4	27.388	35.79	22.15	26.32	23.97	15.4	27.389
L6	51.88	31.23	25.9	45.763	51.88	31.23	54.10	30.18	25.9	45.764
L7	71.90	7.16	9.2	17.672	71.90	7.16	71.49	6.68	9.2	17.672
L8	62.33	7.604	29.5	11.2973	62.33	7.604	63.45	10.88	29.5	11.297

Table 5: The optimal generation and load levels in MW for the IEEE 14-bus system, with smooth and nonsmooth generation cost curves and with/without optimal location/sizing of TCSC and SSSC devices for cases A1–A8.

Generator	Smooth generation cost curve						Nonsmooth generation cost curve			
	Proposed method				SQP [25]		Proposed method			
	Without line flow constraints and without FACTS	With line flow constraints and without FACTS	With line flow constraints and with TCSC	With line flow constraints and with SSSC	Without line flow constraints and without FACTS	With line flow constraints and without FACTS	Without line flow constraints and without FACTS	With line flow constraints and without FACTS	With line flow constraints and with TCSC	With line flow constraints and with SSSC
G1	94.22	97.25	88.84	90.17	100	88.15	90.08	90.64	88.84	90.17
G2	100	100	100	100	100	100	100	100	100	100
G3	100	100	100	100	100	100	100	100	100	100
G4	92.83	48.9	63.59	60.96	92.38	62.88	91.83	46.26	63.59	60.962
L1	58.10	116.90	107.7	108.7	58.10	116.90	55.15	121.01	107.7	108.72
L2	55.63	125.14	116.2	99.778	55.63	125.14	52.49	112.86	116.2	99.778
L3	5.63	8.02	5	12.731	5.63	8.02	5.02	5.94	5	12.731
L4	21.54	16.86	26.8	15.844	21.54	16.86	29.73	16.08	26.8	15.8441
L5	35.79	22.15	15.4	27.388	35.79	22.15	26.32	23.97	15.4	27.389
L6	51.88	31.23	25.9	45.763	51.88	31.23	54.10	30.18	25.9	45.764
L7	71.90	7.16	9.2	17.672	71.90	7.16	71.49	6.68	9.2	17.672
L8	62.33	7.604	29.5	11.2973	62.33	7.604	63.45	10.88	29.5	11.297

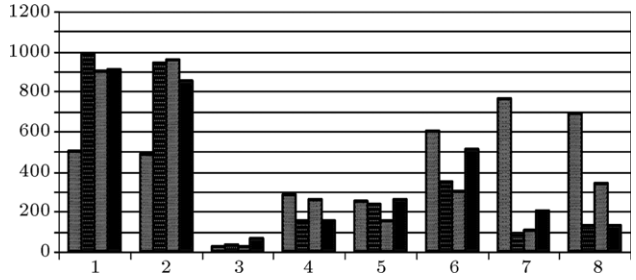

Figure 12: Impact of line flow constraints, TCSC and SSSC, on the individual welfare of each market participant in the modified IEEE 14-bus test system (nonsmooth generation cost curve). (a) Without line flow constraints and without FACTS; (b) with line flow constraints and without FACTS; (c) with line flow constraints and with TCSC; (d) with line flow constraints and with SSSC.

5–8, have greater access to generation buses, and transmission line constraints cannot reduce the amount of their demand. In addition, the generation level of generator G4 (located at bus 6) is decreased and, therefore, total system generation cost is increased (Table 5, row 17).

Enforcement of transmission line constraints (Eq. (23)) alleviates congestion on the transmission lines. However, as expected, line flow constraints cause a significant decrease in social welfares (Table 3).

The main cause of this reduction in the modified IEEE 14-bus test system is reduction of the amount of total load system from 362.84 to 335.08 MW/h, due to transmission line flow constraints. In addition, the total generation and load decrease from 381.9 MW/h and 357.7 MW/h to 336.9 MW/h and 327.64 MW/h for nonsmooth cost curves, respectively.

Regarding the strong structure of the modified IEEE 30-bus test system, after enforcement of transmission line constraints, total system load remains at its maximum value (Table 7). However, increased generation costs reduce total system social welfare.

According to Table 6, in the modified IEEE 30-bus test system without line flow constraints, generators G1, G2, G3 and G8 are lightly loaded, while generators G5, G6 and G7 are reaching maximum capacity. This is due to the different cost benefit coefficients (Eq. (14)). With line constraints, the level of G7 is substantially decreased to about 60 MW. This is the maximum

Table 6: The optimal generation and load levels in MW for the IEEE 30-bus system with smooth and nonsmooth generation cost curves and with/without optimal location/sizing of TCSC and SSSC devices for cases B1–B8.

Generator	Smooth generation cost curve						Nonsmooth generation cost curve			
	Proposed method				SQP [25]		Proposed method			
	Without line flow constraints and without FACTS	With line flow constraints and without FACTS	With line flow constraints and with TCSC	With line flow constraints and with SSSC	Without line flow constraints and without FACTS	With line flow constraints and without FACTS	Without line flow constraints and without FACTS	With line flow constraints and without FACTS	With line flow constraints and with TCSC	With line flow constraints and with SSSC
G1	10	10	10.14	10.18684	10	10	10	10	10	10
G2	5	5	5.02	5.020449	5	5	5	5	5	5
G3	5	5.01	5.04	5	5	5	5	5.06	5	5
G4	29.50	53.94	10	25.90976	25.17	50.82	29.50	54.86	10	27.56258
G5	50	46.83	47.38	47.90413	50.00	50.00	50	48.67	42.26	49.82326
G6	50	48.06	46.75	47.64413	50.00	50.00	50	47.70	44.99	45.13571
G7	100	58.23	92.07	89.75121	100.00	59.98	100	57.87	97.88	90.0211
G8	10	21.44	36.13	23.76607	10	10	10	27.87	38.91	23.56861
G9	27.80	37.73	35.65	29.16266	31.57	45.18	27.80	29.17	35.40	28.92845

Table 7: System analysis results for the IEEE 30-bus test systems with smooth cost curves (powers are in MW).

Case	Smooth generation cost curve				Nonsmooth generation cost curve			
	Operation with TCSC		Operation with SSSC		Operation with TCSC		Operation with SSSC	
	Total generation	Total load	Total generation	Total load	Total generation	Total load	Total generation	Total load
A	352.44	335.70	366.11	352.44	351.86	335.70	351.86	335.70
B	288.46	283.40	286.42	283.40	289.46	283.40	285.04	283.40
C	289.24	283.40	286.78	283.40	289.03	283.40	284.91	283.40
D	290.27	283.40	286.47	283.40	289.30	283.40	283.83	283.40
E	323.55	317.20	321.07	317.20	323.27	317.20	318.41	317.20

capacity of the lines connected to this generator at node 1. In contrast to G7, loading levels of G4, G8 and G9 are significantly increased to fulfill load requirements. As a result, overall social benefit is decreased (Table 7).

8.3. Operation with TCSC/SSSC

According to the previous section, ISO cannot achieve maximum social welfare just by rescheduling generators or load shedding. Therefore, ISO needs to encourage competition, reduce waste, and decrease costs by including FACTS devices.

TCSC and SSSC can be used to transfer power from generators to consumers through un-congested transmission line(s). In this paper, the location and size of TCSC or SSSC units are determined by maximizing the total system social welfare function using Eq. (11).

Simulation results (Table 8 and Figure 12) for all cases show that after TCSC/SSSC compensation, social benefits increase and total generation costs decrease for both smooth and nonsmooth cost curves.

This demonstrates the effectiveness of the sizing and placement of TCSC/SSSC. Optimal locations and sizes of TCSC and SSSC devices, in both smooth and nonsmooth generation cost curves, for the modified 14-bus and 30-bus test systems, are shown in Table 9.

In addition, this table shows the social welfare improvement and TCSC and SSSC comparisons, before and after optimal locating and sizing. According to Table 8 and columns 5 and 9 in Table 9, using both smooth and nonsmooth generation cost curves for all cases, it is seen that SSSC is more efficient than TCSC for increasing social welfare.

Figure 12 shows the individual welfare of each consumer without/with the line flow constraints, and the impact of TCSC/SSSC units (including best location and size) on social benefit, considering nonsmooth cost curves. It is shown that the placement and sizing of TCSC increases the amount of social welfare in loads of 2, 4, 7 and 8. Similarly, SSSC boosts social welfare in loads 3, 5, 6 and 7, significantly. These are caused by allowing more power to reach consumers, due to the optimal locating and sizing of TCSC/SSSC. Furthermore, according to Figure 12, the effects of TCSC and SSSC are the same as for load 1. However, the effects of SSSC on social welfare in loads 3, 5, 6 and 7 are more than TCSC. It is seen that the benefits are not uniformly distributed, i.e., some participants may experience reductions in their welfare/profit.

Obtained results on the modified IEEE 14-bus test system are analyzed as follows:

- According to Table 8 (row 1), the best sizing and placement of TCSC/SSSC will decrease generation costs. The main reason for this is the increase in load demands at nodes 11–14. Therefore, the best placement/sizing of TCSC and SSSC has proven to be beneficial for the IEEE 14-bus test system.
- Furthermore, after placement of TCSC or SSSC, load levels at nodes 4 and 5 (corresponding to loads 1–2), previously elevated due to the line flow constraints, are now decreased (Table 2, row 8 and 9). This is due to their lower benefit coefficients compared to the other loads.
- In addition, according to columns 2 and 4 in Table 8, it can be seen that, by using SSSC instead of TCSC, the generation value increases from 352.44 to 366.11 MW/h, using smooth generation cost curves. In addition, it causes social welfare boosting from 1604.57 to 1660.32 $/h in smooth cases, and augments the amount of 1595.32 to 1648.567 $/h in nonsmooth cases.

Table 8: Cost-benefit analysis by the proposed Fuzzy-GA for the modified IEEE 14-bus and IEEE 30-bus systems with smooth and nonsmooth cost curves.

Case	Smooth generation cost curve						Nonsmooth generation cost curve					
	Operation with TCSC			Operation with SSSC			Operation with TCSC			Operation with SSSC		
	Social benefit ($/h)	Generation cost ($/h)	Customer benefit ($/h)	Social benefit ($/h)	Generation cost ($/h)	Customer benefit ($/h)	Social benefit ($/h)	Generation cost ($/h)	Customer benefit ($/h)	Social benefit ($/h)	Generation cost ($/h)	Customer benefit ($/h)
A	1604.57	1436.26	3040.83	1660.32	1428.59	3088.92	1595.32	1445.51	3040.83	1648.567	1440.35	3088.92
B	7991.08	6233.94	14225.03	8060.45	6164.45	14225.0	7956.55	6268.47	14225.03	8046.18	6178.84	14225.0
C	7901.07	6323.95	14225.03	7899.47	6324.36	14225.0	7878.03	6347.00	14225.03	7879.57	6340.94	14225.0
D	8227.21	5977.90	14225.03	8346.19	5878.84	14225.0	8201.16	6023.86	14225.03	8337.63	5887.39	14225.0
E	8330.33	6874.42	15204.76	8401.94	6802.81	15204.7	8323.77	6880.98	15204.76	8390.140	6814.62	15204.7

Table 9: Best location, parameters and cost of TCSC and SSSC devices versus social welfare improvement in the IEEE 30-bus system with smooth/nonsmooth generation cost curves.

Case		With TCSC				With SSSC				
		Location	Compensation rate % (%)	Improvement in social welfare ($/h)	Cost of TCSC($/h)	Location	Voltage (P.u)	Angel (deg.)	Improvement in social welfare ($/h)	Cost of SSSC ($/h)
A	Smooth cost curve	Line 6–13	25.445	80.65	0.52029	Line 6–13	0.0747	37.583	136.399	0.956231
	Nonsmooth cost curve	Line 6–13	25.305	65.65	0.5049	Line 6–13	0.0713	39.113	118.897	0.915242
B	Smooth cost curve	Line 1–2	58.74	187.41	0.7634	Line 1–2	0.06124	42.850	256.78	0.775313
	Nonsmooth cost curve	Line 1–2	66.97	161.65	0.8704	Line 1–2	0.0607	43.017	251.28	0.750544
C	Smooth cost curve	Line 1–2	55.87	133.07	0.7261	Line 1–2	0.0587	41.458	131.47	0.706241
	Nonsmooth cost curve	Line 1–2	56.61	124.26	0.7357	Line 1–2	0.0572	38.958	125.8	0.694154
D	Smooth cost curve	Line 1–2	61.17	1072.40	0.7950	Line 1–2	0.0672	43.136	1191.36	0.853151
	Nonsmooth cost curve	Line 1–2	61.02	1053.90	0.7931	Line 1–2	0.0657	45.606	1190.38	0.845542
E	Smooth cost curve	Line 1–2	45.22	252.68	0.5877	Line 1–2	0.0591	41.063	324.29	0.719540
	Nonsmooth cost curve	Line 1–2	44.67	271.16	0.5806	Line 1–2	0.0598	44.513	337.53	0.723625

Likewise, results on the modified IEEE 30-bus test system are analyzed as follows:

- After the placement and sizing of TCSC/SSSC, generation of G7 is increased significantly (to transfer more power from node 1 to node 2), which reduces generation costs and increases social benefits (Table 8). These results demonstrate the ability of TCSC/SSSC in improving system operation with line flow constraints.
- Comparing the results of using TCSC and SSSC in Table 6 shows that the amount of total generation and total demand levels in all studied cases (B1–E8) has not changed much. This indicates that the systems under consideration have the capability of supporting maximum loads under assumed congestion conditions. However, according to the results in Table 5 (Cases B1–B8), it is seen that using SSSC and TCSC causes a change in individual generator levels. It causes the decrease of total generation costs from 6233.94 to 6164.45 in cases B5 and B7, using smooth generation cost curves. Similarly, in the case of nonsmooth generation cost curves, the social welfare boost from 7991.08 to 8060.45 $/h (cases B6 and B8) increases. These results indicate that using SSSC is more efficient compared to TCSC.
- In cases C1–C8, line 2–4 is not available and, because of physical limitations on lines 1–2 and 1–3, generator G7 (at bus 1) will not be operating at an optimal point. Therefore, ISO needs to reschedule other generators. According to Table 8 (row 3, column 8), after rescheduling, social welfare by nonsmooth cost curves is improved to 7878 $/h. This is done by placement of TCSC at line 1–2 with a composition level of 56.61% (Table 9; row 6). Similarly, by the best placement of SSSC at line 1–2, which is compensated by a voltage series of 0.0572 pu∠38.95°, social welfare improves to 7879.57 $/h. Therefore, in this case, TCSC and SSSC influences on social welfare improvement are similar. However, it is seen that using SSSC is more economic than TCSC, because in this case, the investment cost of SSSC is less than that of TCSC (Table 9: row 6, columns 6 and 11).

8.4. Economical analysis of using TCSC/SSSC

To investigate the impact of a TCSC and a SSSC on social welfare improvement, their costs are compared with social welfare improvement, in Table 9. According to this table, achieved social welfare improvement using TCSC and SSSC are 80.65 $/h and 136.399 $/h, while the costs of TCSC and SSSC are only 0.52 $/h and 0.956 $/h, respectively. Therefore, investment costs of TCSC and SSSC are significantly less than the improvement in social welfare. Consequently, TCSC and SSSC will increase overall social welfare, although some participants may have more benefit than others.

8.5. Impact of valve point-loading effects on social welfare

In the Modified IEEE 30-bus test system, all loads are nearly at their maximum levels, due to their high cost benefit coefficients (Eq. (12)), as well as system ability in fulfilling load demands. Therefore, it is easy to investigate the impact of generator curves.

- According to Table 8, inclusion of the sin component on the generator's characteristics increases total generation costs and decreases total system social welfare.
- In addition, considering valve point loading effects in the objective function changes the size and investment costs of the TCSC/SSSC and affects the amount of social welfare.

Table 10: Required CPU time (in seconds) and number of iterations (N_{it}) for best location and sizing of TCSC and SSSC devices using GA and the proposed Fuzzy-GA approaches for the studied cases (Table 2).

Case		Smooth cost curve				Nonsmooth cost curve			
		CPU time		Iteration number		CPU time		Iteration number	
		GA	Fuzzy-GA	GA	Fuzzy-GA	GA	Fuzzy-GA	GA	Fuzzy-GA
TCSC	A	489	431 (−11.86%)	609	315 (−48%)	1492	1108 (−25.73%)	619	411 (−33%)
	B	1754	1429 (−18.53%)	729	419 (−42%)	3957	3254 (−17.76%)	682	476 (−30%)
	C	1869	1573 (−15.83%)	745	426 (−42%)	4121	3156 (−23.41%)	703	416 (−40%)
	D	1836	1548 (−15.68%)	732	467 (−36%)	4078	3017 (−26.01%)	725	438 (−39%)
	E	1895	1601 (−15.51%)	751	397 (−47%)	4327	3261 (−24.63%)	691	481 (−30%)
SSSC	A	527	422 (−19.92%)	671	328 (−51%)	1560	1279 (−18.01%)	701	375 (−46%)
	B	1839	1445 (−21.42%)	667	353 (−47%)	4101	3115 (−24.04%)	743	360 (−51%)
	C	1915	1519 (−20.67%)	659	374 (−43%)	4367	3007 (−31.14%)	703	401 (−43%)
	D	1875	1618 (−13.70%)	691	353 (−48%)	4292	3157 (−26.44%)	739	376 (−48%)
	E	1943	1661 (−14.51%)	638	362 (−43%)	4431	3675 (−17.06%)	725	390 (−46%)

Therefore, the ISO needs to consider the actual valve setting points in the objective function by including nonsmooth characteristics to get results that are more accurate and create realistic costs (Table 9).

8.6. Comparing CPU time and number of required iterations

The required number of iterations and processing of CPU time for the best location and sizing of TCSC and SSSC devices for all simulated cases are presented in Table 10. The integration of fuzzy rules in the genetic algorithm has considerably improved convergence characteristics (e.g., requiring 30%–51% less number of iterations and 11%–31% less time for processing).

9. Conclusions

A fuzzy-based genetic algorithm is proposed and implemented to maximize social welfare and perform congestion management in a double-sided auction market, by the best location and sizing of TCSC and SSSC devices and the optimal rescheduling of generation and demand levels. The valve point loading effects are included in the quadratic smooth generator cost curves to establish more accurate models. Adding the sine part in the objective function significantly increases the degree of complexity and the difficulty of detecting the global solution. To guarantee that locational marginal prices charged at the demand buses are less than, or equal to, DisCos benefits, quadratic consumer benefit functions are incorporated into the objective function. Fuzzy rules are integrated in GA to reduce calculation time and iteration numbers for smooth and nonsmooth generator cost curves. In addition, TCSC and SSSC investment costs versus their economical benefits on power systems are discovered. Numerous cases are studied to show the ability of detecting best solutions using the proposed method. The sequential quadratic programming and simple GA outcomes are compared with the proposed method. Based on simulation results for the modified IEEE 14-bus and 30-bus test systems:

- TCSC and SSSC have the ability to redistribute power flow, influence load and generation levels at different buses, and significantly increase social benefits (Tables 7–9). Installation of TCSC/SSSC offers benefits that exceed costs for the system conditions studied.
- TCSC and SSSC devices have different impacts on the welfare of individual participants and may affect the double-sided auction price of each bus differently. Therefore, some participants may benefit more than others (Figure 12).

Table A.1: Characteristics of the GenCos in the modified IEEE 14-bus.

GenCos	1	2	3	4	5
e	50	40	0	0	0
f	0.063	0.098	0	0	0

Table A.2: Characteristics of the GenCos in the modified IEEE 30-bus.

GenCos	1	2	3	4	5	6	7	8	9
e	50	40	0	0	0	0	50	40	0
f	0.063	0.098	0	0	0	0	0.063	0.098	0

- The proposed method shows the benefits of TCSC and SSSC in a deregulated power market and demonstrates how they may be utilized by ISO to improve total system social welfare and prevent congestion.
- The benefits of using TCSC/SSSC may not be considerable at low levels of demand and generation. Simulation studies over an extended period of time would be required to evaluate the overall benefits of TCSC/SSSC for an actual system.
- The smoothness of the generator cost curves shows no significant impact on line overloading; however, it will increase generation costs. This needs to be considered by ISO to get more accurate results and realistic cost analysis.
- Compared to other optimization techniques, such as SQP and GA, the proposed Fuzzy-GA achieves better solutions without/with TCSC/SSSC (Tables 3–4).
- The integration of fuzzy rules in the genetic algorithm will considerably improve convergence and can reduce the number of iterations up to 51% (Table 10). It will also reduce CPU time by about 31% (Table 10).

Appendix

The nonsmooth cost coefficients (Eq. (10)) are presented in Tables A.1 and A.2. The test systems data is presented in [25].

References

[1] Weber, J.D. and Overbye, T.J. "An individual welfare maximization algorithm for electricity markets", *IEEE Trans. Power Syst.*, 17(3), pp. 590–596 (2002).
[2] Choi, J.Y., Rim, S.-H. and Park, J.-K. "Optimal real time pricing of real and reactive powers", *IEEE Trans. Power Syst.*, 13(4), pp. 1226–1231 (1998).
[3] Latorre, G., Cruz, R.D., Areiza, J.M. and Villegas, A. "Classification of publications and models on transmission expansion planning", *IEEE Trans. Power Syst.*, 18(2), pp. 938–946 (2003).

[4] Fonseka, P.A.J. and Shrestha, G.B. "Network expansion under frameworks of regulated monopoly and merchant transmission", *IEEE Singapore Power Tech. Conf.*, 2, pp. 1716–1721 (2004).
[5] Buygi, M.O., Balzer, G., Shanechi, H.M. and Shahidehpour, M. "Market-based transmission expansion planning", *IEEE Trans. Power Syst.*, 19(4), pp. 2060–2067 (2004).
[6] Gautam, D. and Mithulananthan, N. "Locating distributed generator in the LMP-based electricity market for social welfare maximization", *Electr. Power Compon. Syst.*, 35(5), pp. 489–503 (2007).
[7] Hongrui, L., Yanfang, S., Zabinsky, Z.B., Chen-Ching, L., Courts, A. and Sung-Kwan, J. "Social welfare maximization in transmission enhancement considering network congestion", *IEEE Trans. Power Syst.*, 23(3), pp. 1105–1114 (2008).
[8] Gerbex, S., Cherkaoui, R. and Germond, A.J. "Optimal location of multi-type FACTS devices in a power system by means of genetic algorithms", *IEEE Trans. Power Syst.*, 16(3), pp. 537–544 (2001).
[9] Ippolito, L., La Cortiglia, A. and Petrocelli, M. "Optimal allocation of FACTS devices by using multi-objective optimal power flow and genetic algorithms", *Int. J. Emerg. Electr. Power Syst.*, 7(2), Article 1 (2006).
[10] Verma, S.K., Singh, S.N. and Gupta, H.O. "Location of unified power flow controller for congestion management", *Electr. Power Syst. Res.*, 58(2), pp. 89–96 (2001).
[11] Singh, S.N. and David, A.K. "Optimal location of FACTS devices for congestion management", *Electr. Power Syst. Res.*, 58(2), pp. 71–79 (2001).
[12] Zhang, J. and Yokoyama, A. "Optimal power flow control for congestion management by interline power flow controller (IPFC)", *International Conference on Power System Technology*, pp. 1–6 (2006).
[13] Acharya, N. and Mithulananthan, N. "Locating series FACTS devices for congestion management in deregulated electricity markets", *Electr. Power Syst. Res.*, 77(3–4), pp. 352–360 (2007).
[14] Mithulananthan, N. and Acharya, N. "A proposal for investment recovery of FACTS devices in deregulated electricity markets", *Electr. Power Syst. Res.*, 77(5–6), pp. 695–703 (2007).
[15] Shrestha, G.B. and Feng, W. "Effects of series compensation on spot price power markets", *Electr. Power Syst. Res.*, 27(5–6), pp. 428–436 (2005).
[16] Yankui, Zhang and Yan, Zhang "A novel power injection model of embedded SSSC with multi-control modes for power flow analysis inclusive of practical constraints", *Electr. Power Syst. Res.*, 76(4), pp. 374–381 (2006).
[17] Attaviriyanupap, P. and Yokoyama, A. "Economic benefit comparison between series FACTS device installation and new transmission line investment in the deregulated power system using probabilistic method", *9th International Conference on Probabilistic Methods Applied to Power Systems KTH*, Stockholm, pp. 1–7 (2006).
[18] Singh, K., Padhy, N.P. and Sharma, J.D. "Social welfare maximization considering reactive power and congestion management in the deregulated environment", *Electr. Power Compon. Syst.*, 38(1), pp. 50–71 (2010).
[19] AlRashidi, M.R. and El-Hawary, M.E. "Hybrid particle swarm optimization approach for solving the discrete OPF problem considering the valve loading effects", *IEEE Trans. Power Syst.*, 22(4), pp. 2030–2038 (2007).
[20] Wang, X.P. and Cao, L.P. "Genetic algorithms—theory, application and software realization", Xi'an Jiaotong University, Xi'an, China (1998).
[21] Ulinuha, A., Masoum, M.A.S. and Islam, S.M. "Optimal scheduling of LTC and shunt capacitors in large distorted distribution systems using genetic algorithms", *IEEE Trans. Power Deliv.*, 23(1), pp. 434–441 (2008).
[22] Masoum, M.A.S., Ladjevardi, M., Jafarian, A. and Fuchs, E.F. "Optimal placement, replacement and sizing of capacitor banks in distorted distribution networks by genetic algorithms", *IEEE Trans. Power Deliv.*, 19(4), pp. 1794–1801 (2004).
[23] Shi, Y., Eberhart, R. and Chen, Y. "Implementation of evolutionary fuzzy systems", *IEEE Trans. Fuzzy Syst.*, 7(2), pp. 109–119 (1999).
[24] Shiddehpour, M., Yamin, H. and Li, Z.Y., *Market Operations in Electric Power System*, Wiley, New York pp. 477–478 (2002).
[25] Zimmerman, R.D., Murillo-Sanchez, C.E. and Gan, D. "MATPOWER: a matlab power system simulation package" [Online] (2006). Available: http://www.pserc.cornell.edu/matpower.

Seyyed Mohammad Hossein Nabavi (M'10) received his B.S. (Honors) degree and M.S. (Honors) degree in Electrical and Computer Engineering in 1998 and 2001, respectively, from the Iran University of Science and Technology, Tehran, Iran, where he is currently a Ph.D. degree student. His research interests include optimization, power system operation and control. He has been a member of IEEE since 2010.

Ahad Kazemi received his M.S. degree in Electrical Engineering from Oklahoma State University, USA in 1979. He is currently Associate Professor at the Electrical Engineering Department of Iran University of Science and Technology, Tehran, Iran. His research interests are: reactive power control, power system dynamics, stability and control of FACTS devices.

Mohammad Ali Sherkat Masoum (SM'05) received his B.S., M.S. and Ph.D. degrees in Electrical and Computer Engineering in 1983, 1985, and 1991, respectively, from the University of Colorado at Boulder, USA. Currently, he is Associate Professor in the Department of Electrical and Computer Engineering at Curtin University of Technology, Perth, Australia.